Research Article

NEURAL REGENERATION RESEARCH
www.nrronline.org

An enriched environment reduces hippocampal inflammatory response and improves cognitive function in a mouse model of stroke

https://doi.org/10.4103/1673-5374.338999

Date of submission: August 31, 2021

Date of decision: November 29, 2021

Date of acceptance: December 28, 2021

Date of web publication: April 1, 2022

Hong-Yu Zhou[1, #], Ya-Ping Huai[2, #], Xing Jin[1], Ping Yan[3], Xiao-Jia Tang[1], Jun-Ya Wang[1], Nan Shi[3], Meng Niu[4], Zhao-Xiang Meng[1, *], Xin Wang[1, *]

From the Contents

Introduction	2497
Materials and Methods	2498
Results	2499
Discussion	2499

Graphical Abstract *Enriched and isolated environments can regulate the TRAF6/NF-κBp65 signaling pathway in the hippocampus through miR-146a-5p and affect cognitive function in a stroke mouse model*

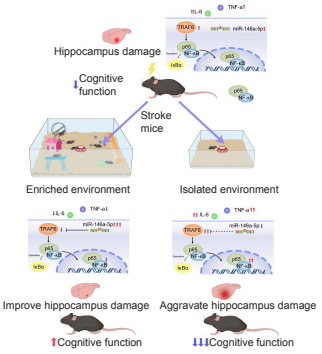

Abstract

An enriched environment is used as a behavioral intervention therapy that applies sensory, motor, and social stimulation, and has been used in basic and clinical research of various neurological diseases. In this study, we established mouse models of photothrombotic stroke and, 24 hours later, raised them in a standard, enriched, or isolated environment for 4 weeks. Compared with the mice raised in a standard environment, the cognitive function of mice raised in an enriched environment was better and the pathological damage in the hippocampal CA1 region was remarkably alleviated. Furthermore, protein expression levels of tumor necrosis factor receptor-associated factor 6, nuclear factor κB p65, interleukin-6, and tumor necrosis factor α, and the mRNA expression level of tumor necrosis factor receptor-associated factor 6 were greatly lower, while the expression level of miR-146a-5p was higher. Compared with the mice raised in a standard environment, changes in these indices in mice raised in an isolated environment were opposite to mice raised in an enriched environment. These findings suggest that different living environments affect the hippocampal inflammatory response and cognitive function in a mouse model of stroke. An enriched environment can improve cognitive function following stroke through up-regulation of miR-146a-5p expression and a reduction in the inflammatory response.

Key Words: cognitive function; enriched environment; isolated environment; miR-146a-5p; neuroinflammation; nuclear factor κB p65; photothrombotic model; stroke; tumor necrosis factor receptor-associated factor 6

Introduction

Stroke, the second leading cause of death in the world, is a common acute cerebrovascular disease (Xie et al., 2019), and approximately 80% of cases of stroke are ischemic (Faralli et al., 2013). Studies have found that approximately 50% of patients with stroke have varying degrees of cognitive dysfunction (Sachdev et al., 2006; Mijajlović et al., 2017; Zhang and Bi, 2020), which severely affects patients' quality of life and survival time. In clinical practice, most patients with stroke do not like to talk to others, lack subjective initiative, and spend most of their time alone, all of which seriously affect the recovery of neurocognitive function. One study has shown that isolated housing can lead to poor recovery and microRNA (miRNA) imbalance, and decrease hippocampal cell proliferation in older female mice models of stroke (Holmes et al., 2020). Therefore, interventions related to the cognitive function of patients with stroke have become a research hot spot.

An enriched environment (EE) is a special environment that can enhance sports ability, cognition, perception, and social interaction (Will et al., 2004). Animal studies have shown that an EE not only improves learning, cognitive,and sports abilities in normal animals, but also improves the cognitive and sports abilities of rats with various central nervous system diseases (Hockly et al., 2002; Bezard et al., 2003; Restivo et al., 2005; Kovesdi et al., 2011). EE is currently used in the clinical rehabilitation of patients with stroke (White et al., 2015), but the specific mechanism underlying its positive effect remains unclear. Our previous study found that an EE can improve post-stroke cognitive impairment (PSCI) by regulating acetylation homeostasis in the cholinergic circuit in mouse models of stroke (Wang et al., 2016). The occurrence of PSCI is closely related to factors such as the inflammatory response (Narasimhalu et al., 2015). As an important immune-related molecule, miR-146a plays a key role in both innate immunity and neuroimmunity, and can inhibit the levels of inflammatory factors such as interleukin 6 (IL-6), IL-8, IL-1β, and tumor necrosis factor-α (TNF-α) by down-regulating tumor necrosis factor receptor-associated factor 6 (TRAF6) expression (Lukiw et al., 2008; Aronica et al., 2010).

Therefore, in this study, photothrombotic stroke mouse models were rehabilitated in either EE or isolated environments. Due to the mutual

[1]Department of Rehabilitation Medicine, Northern Jiangsu People's Hospital Affiliated to Yangzhou University (Clinical Medical College, Yangzhou University), Yangzhou, Jiangsu Province, China; [2]Department of Rehabilitation Medicine, Shenzhen Longhua District Central Hospital, Shenzhen, Guangdong Province, China; [3]School of Nursing, Yangzhou University, Yangzhou, Jiangsu Province, China; [4]Dalian Medical University, Dalian, Liaoning Province, China

***Correspondence to:** Xin Wang, PhD, wx000805qm@yeah.net; Zhao-Xiang Meng, PhD, yzmzx001@163.com.

https://orcid.org/0000-0003-1961-9615 (Xin Wang); https://orcid.org/0000-0001-9624-2829 (Zhao-Xing Meng)

#Both authors contributed equally to this article.

Funding: *This study was financially supported by the National Natural Science Foundation of China, No. 82072533, the China Postdoctoral Science Foundation, No. 2017M621675, Huxin Foundation of Jiangsu Key Laboratory of Zoonosis of China, No. HX2003; and Yangzhou Science and Technology Development Plan Project of China, No. YZ2020201 (all to XW).*

How to cite this article: *Zhou HY, Huai YP, Jin X, Yan P, Tang XJ, Wang JY, Shi N, Niu M, Meng ZX, Wang X (2022) An enriched environment reduces hippocampal inflammatory response and improves cognitive function in a mouse model of stroke. Neural Regen Res 17(11):2497-2503.*

interaction between miR-146a-5p and neuroinflammation, as well as their association with cognitive function, we examined the efficacy of an EE in improving cognitive function after stroke, as well as the mechanism underlying this effect, at the levels of miRNA and neuroinflammation.

Materials and Methods

Photothrombotic stroke models and interventions

The animal experiment was approved by the Animal Ethics Committee of Yangzhou University, China (approval No. 20170312001) in March 2017. We used 92 healthy, male, clean-grade C57BL/6 mice aged 2 months (provided by the Animal Experiment Center of Medical College of Yangzhou University, China; license No. SYXK (Su) 2017-0044). Among them, 70 mice were subjected to photothrombotic stroke. Briefly, after anesthesia (intraperitoneal injection of 1% sodium pentobarbital solution, 0.1 mL/10 g, Cat# P-010, Sigma-Aldrich, St. Louis, MO, USA), Rose Bengal (1%, 1 mg/10 g, Cat# B7767, APExBIO, Houston, TX, USA) was injected intraperitoneally. The mouse was placed in the prone position, the tops of their heads were shaved, and the scalp was cut along the midline to fully expose the bregma (Watson et al., 1985; Labat-gest and Tomasi, 2013). The cold light source probe (Cat# ULP-L20-S, Bete Jia, Suzhou, China) was placed approximately 2 mm below the left of the bregma. After 5 minutes of Rose Bengal injection, the cold light source was turned on and irradiation was continued for 15 minutes (Uzdensky, 2018). Four mice died during the modeling process; the 66 surviving mice were divided into the stroke + standard environment (SE) group, stroke + EE group, and stroke + isolated environment (IE) group using a random number table method. Another 22 mice were selected as the sham operation group. In this sham group, 0.9% normal saline (0.1 mL/10 g) was injected intraperitoneally with the same amount of Rose Bengal without light, and the remaining steps were the same as for stroke model mice. Sham group mice (n = 22) were placed in an SE cage for 4 weeks. SE group mice (n = 22) group were also placed in another SE cage for 4 weeks. EE group mice (n = 22) were placed in an EE cage for 4 weeks. IE group mice were individually caged for 4 weeks. The flow chart of this study design is shown in **Figure 1**.

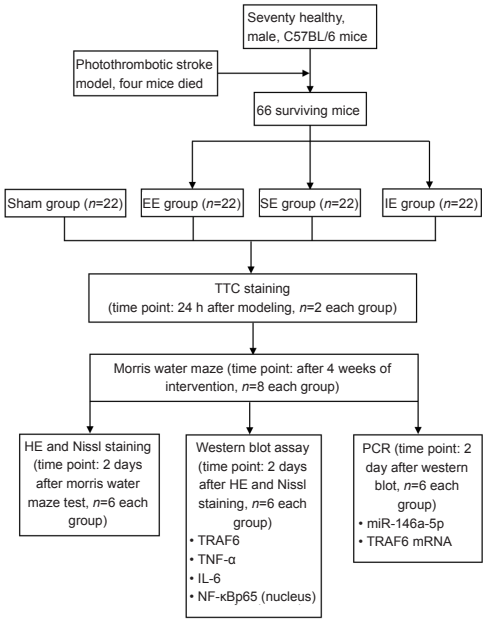

Figure 1 | **Flow chart of this study.**
SE group: Stroke + standard environment group; EE group: enriched environment group; IE group: stroke + isolated environment group; HE: hematoxylin-eosin; TRAF6: factor receptor-associated factor 6; TNF-α: tumor necrosis factor-α; IL-6: interleukin 6; NF-κBp65: nuclear factor kappa-Bp65; TTC: triphenyl tetrazolium chloride; RT-qPCR: real time quantitative polymerase chain reaction.

Construction of mouse cages in different environments

According to our previous research (Wang et al., 2016), the EE cage was improved to comprise a 1.2-m^3 three-layer plexiglass cage. Each floor was connected by a plastic corridor. Inside the EE cage, there were three spiral staircases (each staircase entrance was equipped with rough carpet), three tunnels of different styles, two walking wheel pipes, two turntables, two swings, toy building blocks, a cabin, a bell sound, and color light stimulation. The EE group mice were held in researchers' palms and vigorously brushed from head to tail with a soft brush once a day, and the environment was changed once every 3 days to update the stimulation until the 4th week (**Figure 2A** and **B**). In contrast, the SE cage was 75 × 55 × 35 cm^3, with mouse food, water, and padding (**Figure 2C** and **D**), and the IE cage was 29 × 18 × 16 cm^3, with mouse food, water, and padding (**Figure 2E** and **F**).

Triphenyl tetrazolium chloride staining

At 24 hours after modeling, two mice from each group were selected using the random number table method for mouse brain triphenyl tetrazolium chloride (TTC) staining. The mice were sacrificed under 10% (lethal dose) sodium pentobarbital deep anesthesia. The mice brains were removed and quickly frozen at –20°C for 20 minutes, restored at room temperature for 10 minutes, and then cut into five 2-mm continuous coronal brain slices from the starting point of the optic chiasm toward the caudal side. Following slicing, a newly prepared 2% TTC solution (Servicebio, Wuhan, Hubei Province, China, Cat# G1017) was added, slices were incubated at room temperature for 30 minutes in the dark, and then fixed in a phosphate buffer containing 4% paraformaldehyde overnight. The color of the frontal part of the coronal section of the mouse brain was observed to determine whether the mouse had indeed undergone stroke.

Morris water maze

After 4 weeks of intervention, eight mice in each group were selected for inclusion in the Morris water maze experiment (Shanghai Xinruan Information Technology Co., Ltd., Shanghai, China). The mice were trained from day 1 to day 4 and tested on days 5 and 6. During training and testing, the water temperature was maintained at 20–22°C, and a platform was placed 2 cm below the water level in one of the four quadrants. During training and testing, each group of mice was put into the water from the four quadrant water inlet points. If the mice did not reach the platform within 60 seconds, they were guided to the platform and stayed there for 30 seconds. Additionally, the escape latency of each group was recorded. On day 6, the platform was removed from the pool, and mice were allowed to swim freely for 60 seconds. The video analysis system automatically recorded the number of times mice crossed the platform zone. After the daily tests, mice were returned to their respective environments.

Histological observation

Two days after completion of the Morris water maze test, six mice in each group were deeply anesthetized by intraperitoneal injection of 10% sodium pentobarbital, and brains were removed after cardiac perfusion. The fresh brain tissue was immediately put on ice, and then dehydrated gradually in 15%, 20%, and 30% sucrose solution until the specimen sunk to the bottom. The specimen was then removed from the solution, embedded with optimal cutting temperature embedding agent (Servicebio, Cat# G6059), and placed in a freezing microtome (Dakewe Biotech, Shenzhen, China, Cat# 3000A). When the brain block had frozen solid, it was fixed on a freezing microtome and sliced. Starting from the optic chiasm, a serial section of the coronal position was obtained, with a section thickness of 4 μm. When the hippocampus appeared, the coronal slices of the hippocampi at the same level were selected for hematoxylin-eosin and Nissl staining in each group.

Hematoxylin-eosin staining

The hippocampal sections were laid flat on a glass slide, fixed for 0.5–1 minute, stained with hematoxylin (Servicebio, Cat# G1005) for 3–4 minutes, washed with water to remove the dye on the surface, and tap water was applied for 5 minutes, until all slices turned blue. The slices were then rinsed in distilled water for 2 minutes. Then, the slices were dyed with eosin solution (Servicebio, Cat# G1001) for 30 seconds before removing with 75% alcohol for 1–2 minutes, 95% ethanol for 3 minutes, dehydration of two grades of absolute ethanol for 3 minutes, two grades of xylene for 3 minutes, and finally sealed with neutral gum (Servicebio, Cat# WG10004160). The sealed slide was then placed under an optical microscope (Olympus, Tokyo, Japan, Cat# BX53) to observe and collect images.

Nissl staining

The hippocampal sections in the same location were also laid flat on another glass slide for Nissl staining. Nissl staining solution (Cat# G1036, Servicebio) was added dropwise onto the glass slide, rinsed with distilled water twice after staining for 5 minutes, and shaken to remove excess water. For decolorization, the slides were washed twice with 70% ethanol solution to remove excess color, and the slides were removed from ethanol solution in due course. For dehydration, the slices were transferred to a 95% ethanol solution and dehydrated for 2 minutes; the slides were then switched to a fresh 95% ethanol solution and dehydrated for a further 2 minutes. For transparency, the slices were transferred to fresh xylene solution for 5 minutes. Finally, the slides were sealed with neutral gum. The sealed glass slide was placed under an optical microscope to observe and collect images, and the number of Nissl bodies in the hippocampus CA1 region of the selected mice in each group was counted using ImageJ software version 1.49 (National Institute of Health, Bethesda, MD, USA; Schneider et al., 2012).

Western blot assay

In the absence of stimulation, nuclear factor kappa-Bp65 (NF-κBp65) is sequestered in the cytoplasm by nuclear factor-kappa B inhibitor α (IκB-α). After stimulation, IκBα is phosphorylated, which leads to dissociation of the NF-κB/IκBα complex and translocation of NF-κB in the nucleus (Oeckinghaus and Ghosh, 2009). Therefore, we analyzed the level of NF-κBp65 in the hippocampal nucleus of a mouse model of stroke. Six mice were taken from each group and sacrificed under deep anesthesia by intraperitoneal injection of 10% (lethal dose) sodium pentobarbital. Brain tissue from the left hippocampus area was rapidly isolated on ice, and then thoroughly crushed. The hippocampal whole protein and nucleoprotein protein were respectively extracted from hippocampus by a total protein extraction kit (KeyGen Biotech, Nanjing, China, Cat# KGP250) and nucleoprotein extraction kit (KeyGen Biotech, Cat# KGP150), then analyzed using western blot. The protein mixture was centrifuged at 4°C and 12,000 × g for 30 minutes, and

the supernatant was collected. A bicinchoninic acid kit (Cat# KGPBCA, KeyGen Biotech) was used to detect protein concentration. The samples were heated at 100°C for 10 minutes. The protein samples (20 μL) were subjected to 10% sodium dodecyl sulfate-polyacrylamide gel electrophoresis, and then transferred to a polyvinylidene fluoride membrane (Cat# 1620112, Bio-Rad, Shanghai, China). The polyvinylidene fluoride membrane was then transferred to nonfat milk-blocking solution for 1 hour at room temperature. The primary antibodies used were anti-NF-κBp65 (1:1000, rabbit, Abcam, Cat# ab76302, RRID: AB_1524028), anti-TRAF6 (1:2000, rabbit, Abcam, Cat# ab33915, RRID: AB_778572), anti-TNF-α (1:1000, rabbit, Abcam, Cat# ab183218, RRID: AB_2889388), and anti-IL-6 (1:1000, rabbit, Abcam, Cat# ab229381, RRID: AB_2861234). Anti-glyceraldehyde-3-phosphate dehydrogenase (1:10,000, rabbit, Abcam, Cat# ab181602, RRID: AB_2630358) and anti-histone H3 (1:1000, rabbit, Abcam, Cat# ab215728, RRID: AB_2118291) were used as a loading control. The membranes were incubated overnight with primary antibodies at 4°C. Membranes were then washed three times with Trisbuffered saline with Tween-20. The membrane was then incubated with the IgG secondary antibody (1:5000, rabbit, Abcam, Cat# ab205718, RRID: AB_2819160) for 60 minutes at room temperature. After development, ImageJ software was used to measure the relative optical density of each band.

Quantitative reverse transcription-polymerase chain reaction

The left hippocampus tissues of six mice in each group were collected. An RNA extraction kit (Tiangen, Beijing, China, Cat# DP501) was used to extract total RNA from the hippocampus, and the RNA concentration was detected using a microplate reader (Tecan, Shanghai, China, Cat# M1000). The concentration of each sample to be tested was diluted to 200 ng/μL.

miRNA detection

A 20 μL reaction solution was prepared on ice, comprising total RNA (8 μL), 2× miRNA RT reaction buffer (10 μL), and miRNA RT enzyme mix (2 μL). The reaction mixture was mixed thoroughly, and reverse transcription of miRNA was performed to obtain complementary deoxyribonucleic acid (cDNA). A real-time quantitative polymerase chain reaction (qPCR) plate was used to prepare 20 μL total reaction solution, as follows: 2× miRcute Plus miRNA Premix (with SYBR&ROX; 10 μL), forward primer (10 μM; 0.4 μL), reverse primer (10 μM; 0.4 μL), 50× ROX Reference Dye (2 μL), ddH_2O (5.2 μL), and cDNA (2 μL). The sample was then transferred to a fluorescence qPCR machine (Cat# StepOne Plus 4376357, Thermo Fisher Scientific, Waltham, MA, USA), and the qPCR reaction was performed with the following amplification conditions: 95°C, 15 minutes for 1 cycle; 94°C, 20 seconds; 64°C, 30 seconds; 72°C, 34 seconds for 5 cycles; 94°C, 20 seconds; and 60°C, 34 seconds for 45 cycles. All the reagents were from Tiangen.

mRNA detection

A 20 μL reaction solution was prepared on ice, comprising 5 × FastKing-RT SuperMix (4 μL), RNase-Free ddH_2O (14 μL), and total RNA (2 μL). The sample was mixed well, and reverse transcription of mRNA was performed to obtain cDNA. Subsequently, a 20 μL system total reaction solution was prepared with a qPCR plate, as follows: 2× SuperReal PreMix Plus (10 μL), forward primer (10 μM; 0.6 μL), reverse primer (10 μM; 0.6 μL), cDNA (2 μL), 50× ROX Reference Dye (2 μL), and RNase-free ddH_2O (4.8 μL). The amplification conditions were as follows: 95°C, 15 minutes for 1 cycle; 95°C, 10 seconds; and 63°C, 32 seconds for 40 cycles. All the reagents were from Tiangen.

Primer sequence

miR-146a-5p: forward: 5′-TGC GCT GAG AAC TGA ATT CCA T-3′, reverse: 5′-TGG TGT CGT GGA GTC G-3′; internal reference U6: forward: 5′-CTC GCT TCG GCA GCA CAT-3′, reverse: 5′-AAC GCT TCA CGA ATT TGC GT-3′; TRAF6: forward: 5′-CCA ATT CCC AGA ATC CAG AAA-3′, reverse: 5′-GAC ACA GAG GAC CCA CAG AGA A-3′; internal reference glyceraldehyde-3-phosphate dehydrogenase: forward: 5′-TGA AGG GTG GAG CCA AAA G-3′, reverse: 5′-AGT CTT CTG GGT GGC AGT GAT-3′. The $2^{-\Delta\Delta Ct}$ method (Schmittgen and Livak, 2008) was used to calculate the relative expression levels of miR-146a-5p and TRAF6 mRNA, where $\Delta Ct = Ct_{target\ gene} - Ct_{reference\ gene}$.

Database prediction comparison analysis

By comparing the base sequences of TRAF6 mRNA 3′ untranslated region and miR-146a-5p using Targetscan (http://www.targetscan.org/vert_80/) and Human microRNA disease bioinformatics databases (http://www.cuilab.cn/hmdd/), we were able to determine whether they have complementary regions of base pairs.

Statistical analysis

No statistical methods were used to predetermine sample sizes; however, our sample sizes are similar to those reported in a previous publication (Wang et al., 2016). No animals or data points were excluded from the analysis. The evaluator was blind to the grouping. All data were analyzed using SPSS 23.0 (IBM, Armonk, NY, USA) and GraphPad Prism 8.0 (GraphPad Software Inc., San Diego, CA, USA) statistical software, and the measurement data are expressed as mean ± standard deviation (SD). The Morris water maze data and western blotting data conformed to a normal distribution, so one-way analysis of variance was used for comparisons between multiple groups, and the least significant difference test was used for pairwise comparisons. The qPCR data did not conform to a normal distribution, so nonparametric tests were used (the Kruskal-Wallis test was used for comparisons between multiple groups, and the Mann-Whitney *U* test was used for pairwise comparisons). A *P*-value < 0.05 was taken to indicate statistical significance.

Results

Successful establishment of stroke model

As shown in **Figure 3**, the brain tissue of mice in the sham group was normal with red coloring, while the left cortex and subcortex in mice with photothrombotic stroke were white under TTC staining, which indicates ischemic infarction.

EE improves learning and memory in a mouse model of stroke

The Morris water maze results are shown in **Figure 4**. Compared with the sham group, the escape latency was significantly longer in the SE group from day 3 ($P < 0.05$). Moreover, the escape latency in the EE group was shorter than that of the SE group on days 3–5 ($P < 0.05$). The escape latency was significantly longer in the IE group than in the SE group ($P < 0.05$) on days 4 and 5. On day 6, the SE group made fewer crossings of the platform zone than the sham group ($P < 0.05$). The times of crossing the platform zone in the EE group was higher than that in the SE group ($P < 0.05$), while the number of platform zone crossings in the IE group was less than that in the SE group ($P < 0.05$). The swimming trajectories of each group are shown in **Figure 5**. The results indicated a significant decrease in the learning and memory ability of post-stroke mice in the SE group. The EE could improve the learning and memory ability of mice after stroke, while the IE aggravated the learning and memory impairments of mice after stroke.

EE limits cell damage in the hippocampal CA1 region of a mouse model of stroke

The hematoxylin-eosin and Nissl staining results are shown in **Figure 6**. In the hippocampal CA1 region in the sham group, the nerve cells were neatly arranged, with full cytoplasm, normal morphology, and large, round nuclei that were clearly visible and evenly distributed, and there were abundant Nissl bodies. In the SE group, the cell arrangement was disordered, the intercellular density was decreased and the intercellular space increased, the morphology was abnormal, the cell membrane was ruptured, the nucleus was irregular or pyknotic, there was evidence of neuronal degeneration, and inflammatory cells were infiltrated, and the number of Nissl bodies was less than that in the sham group ($P < 0.05$). The morphology and structure of CA1 cells in the EE group were more complete and clearer, the arrangement was relatively regular, and there were more Nissl bodies than in the SE group ($P < 0.05$). In the IE group, the hippocampal CA1 cells were seriously damaged, with unclear cell structure, deep pyknosis, unclear nucleoli, significantly decreased cell density, and an increase in the number of vacuoles and inflammatory cell infiltration, and the number of Nissl bodies was significantly reduced compared with the SE group ($P < 0.05$). Under the SE condition, hippocampal neurons were damaged after stroke in mice, EE protected hippocampal neurons in mice after stroke, while IE aggravated cell damage in the hippocampal tissue of a mouse model of stroke.

EE decreases the protein expression levels of TRAF6, NF-κBp65 (nuclear), TNF-α, and IL-6 in the injured hippocampus of a mouse model of stroke

Western blot results are shown in **Figure 7**. Compared with the sham group, the protein expression levels of TRAF6, NF-κBp65 (nuclear), TNF-α, and IL-6 in the left hippocampus of the SE group were increased ($P < 0.05$). The protein expression levels of TRAF6, NF-κBp65 (nuclear), TNF-α, and IL-6 in the left hippocampus of the EE group were lower than those in the SE group ($P < 0.05$). The protein expression levels of TRAF6, NF-κBp65 (nuclear), TNF-α, and IL-6 in the hippocampus of the IE group were higher than those in the SE group ($P < 0.05$).

EE affects the expression levels of miR-146a-5p and TRAF6 mRNA in injured hippocampus of a mouse model of stroke

The relative expression levels of miR-146a-5p are shown in **Figure 8**. Compared with the sham group, the expression of miR-146a-5p in the hippocampus of the SE group was increased ($P < 0.05$). Compared with the SE group, the expression of miR-146a-5p in the hippocampus of the EE group was increased ($P < 0.05$), and the expression of miR-146a-5p in the hippocampus of the IE group was decreased ($P < 0.05$).

The relative expression levels of TRAF6 mRNA are shown in **Figure 8**. Compared with the sham group, the expression of TRAF6 mRNA in the hippocampus of the SE group was significantly increased ($P < 0.05$). Compared with the SE group, the TRAF6 mRNA expression in the hippocampus of the EE group was significantly reduced ($P < 0.05$), and the expression of TRAF6 mRNA in the hippocampus of the IE group was significantly increased ($P < 0.05$).

miR-146a-5p targets and regulates TRAF6 mRNA

According to the database prediction comparison analysis, we found that miR-146a-5p targeted TRAF6 mRNA. Multiple sites in the 3′ untranslated region of TRAF6 mRNA that can bind to miR-146a-5p were identified (**Figure 9**).

Discussion

PSCI is a complication of ischemic stroke, and usually manifests as dysfunction of memory, attention, execution, direction, and language (Sun et al., 2014). In addition to the application of drug therapy and traditional cognitive rehabilitation training, the potential of new multi-modal training rehabilitation methods is constantly being explored (Park et al., 2014; Ngandu et al., 2015; Teo et al., 2016; Maresova et al., 2018). Our results demonstrated that EEs and IEs can regulate the TRAF6/NF-κBp65 signaling pathway in the hippocampus of a mouse model of stroke through miR-146a-5p, and affect the morphology and inflammation level of the hippocampus, as well as cognitive function in mice.

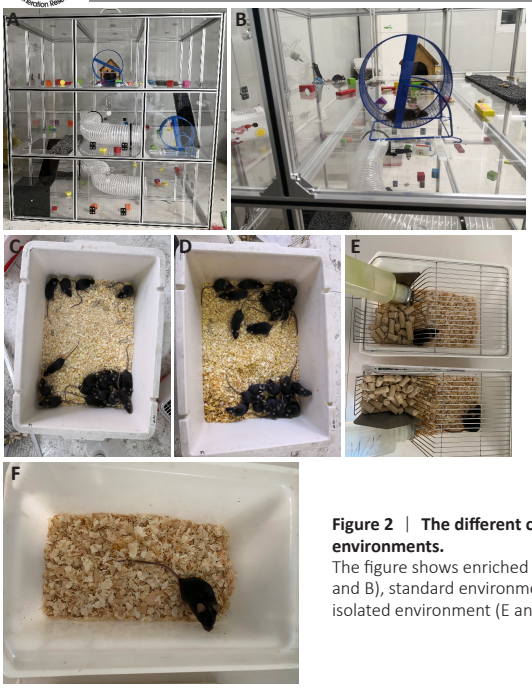

Figure 2 | The different cage environments.
The figure shows enriched environment (A and B), standard environment (C and D), and isolated environment (E and F) cages.

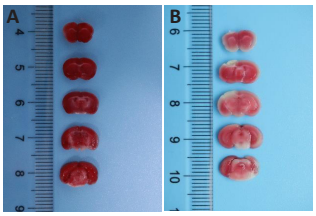

Figure 3 | Triphenyl tetrazolium chloride staining of the brain in control mice (A) and photothrombotic stroke model mice (B).
The non-ischemic necrosis area was red, and the avascular necrosis area was white. The brain tissue of mice in the sham mice was normal with red color (A), while the left cortex and subcortex in mice with photothrombotic stroke were white (B) under triphenyl tetrazolium chloride staining, which suggests ischemic infarction.

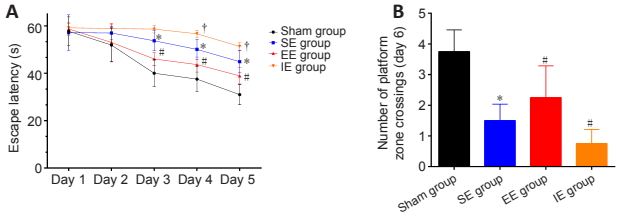

Figure 4 | The enriched environment improved learning and memory of a mouse model of stroke in the Morris water maze.
(A) Average escape latency on days 1–5. (B) The number of platform zone crossings on day 6. Data are expressed as the mean ± SD (n = 8). *P < 0.05, *vs.* sham group; #P < 0.05, *vs.* SE group; †P < 0.05, *vs.* SE group (one-way analysis of variance followed by least significant difference test). EE group: stroke + enriched environment group; IE group: stroke + isolated environment group; SE group: stroke + standard environment group.

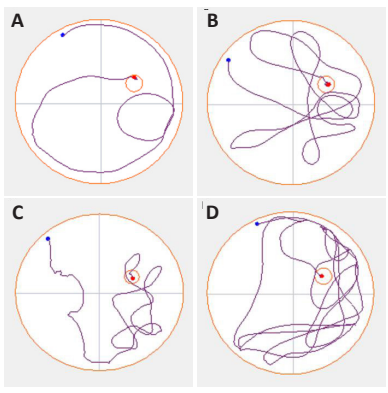

Figure 5 | Effects of the enriched environment on the swimming trajectory of a mouse model of stroke on day 5 of the Morris water maze test.
(A) Sham group. (B) SE group. (C) EE group. (D) IE group. After stroke, the swimming trajectory of the mice looking for the platform was extended. The enriched environment shortened the swimming trajectory of mice, and the isolated environment further extended the swimming trajectory of mice. The blue dot indicates the point at which mice were placed into the water; the red dot indicates the end of the swimming track; the big red circle indicates the edge of the pool; the small red circle indicates the platform. EE group: stroke + enriched environment group; IE group: stroke + isolated environment group; SE group: stroke + standard environment group.

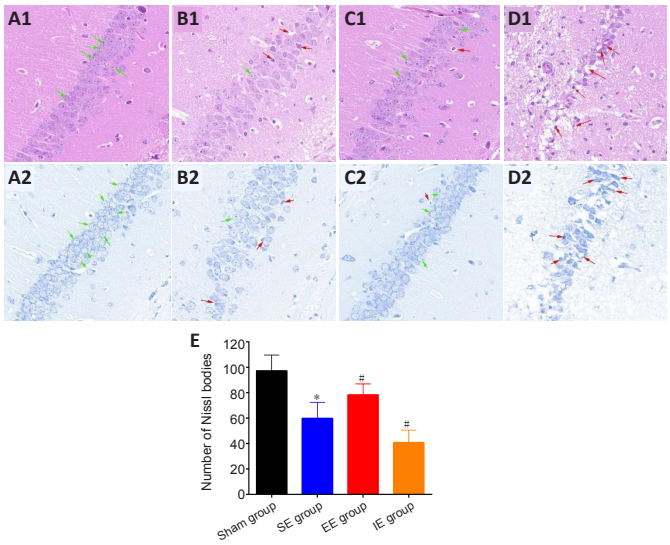

Figure 6 | Effects of the enriched environment on the histopathology in the hippocampal CA1 region of a mouse model of stroke.
(A–D) Hematoxylin-eosin (A1, B1, C1, D1) and Nissl (A2, B2, C2, D2) staining in the hippocampal CA1 region in the sham (A), SE (B), EE (C), and IE (D) groups (original magnification 400×). Red arrows indicate nerve cells that were obviously irregular, with nuclear pyknosis and vacuoles; and green arrows indicate normal nerve cells. The morphology of hippocampal CA1 cells in the sham group was normal, hippocampal CA1 cells in the SE group were damaged, the morphology of CA1 cells in the EE group was improved compared to SE, and hippocampal CA1 cells in the IE group were more damaged compared to SE. (E) Number of Nissl bodies in the hippocampal CA1 region (per 400-fold field). Data are expressed as the mean ± SD (n = 6). *P < 0.05, *vs.* sham group; #P < 0.05, *vs.* SE group (one-way analysis of variance followed by least significant difference test). EE group: stroke + enriched environment group; IE group: stroke + isolated environment group; SE group: stroke + standard environment group.

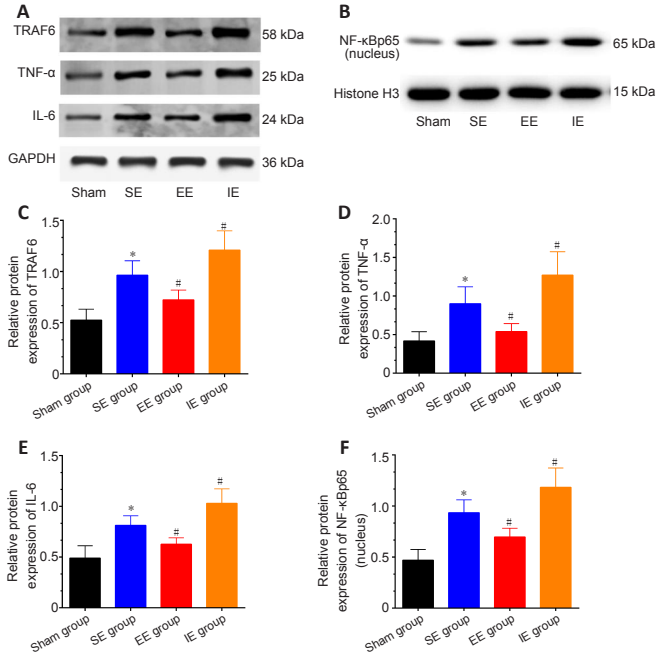

Figure 7 | Effects of the enriched environment on the protein expression levels of TRAF6, NF-κBp65 (nucleus), TNF-α, and IL-6 in the hippocampus of a mouse model of stroke using Western blot assay.
(A) Bands of TRAF6, TNF-α, and IL-6 protein. (B) Bands of NF-κBp65 (nucleus) protein. (C–F) Quantitative results of TRAF6, TNF-α, IL-6, and NF-κBp65 (nucleus) protein expression. The expression of TRAF6, TNF-α, and IL-6 protein was normalized against GAPDH, and the expression of NF-κBp65 (nucleus) protein was normalized against Histone H3. Data are expressed as the mean ± SD (n = 6). *P < 0.05, *vs.* sham group; #P < 0.05, *vs.* SE group (one-way analysis of variance followed by least significant difference test). EE group: stroke + enriched environment group; GAPDH: glyceraldehyde-3-phosphate dehydrogenase; IE group: stroke + isolated environment group; IL-6: interleukin 6; NF-κBp65: nuclear factor kappa-Bp65; SE group: stroke + standard environment group; TNF-α: tumor necrosis factor-α; TRAF6: factor receptor-associated factor 6.

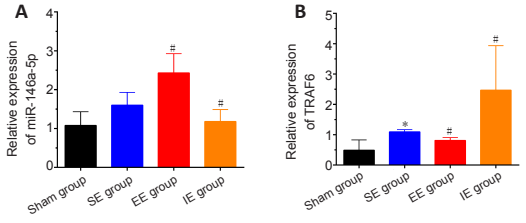

Figure 8 | Effects of the enriched environment on the expression levels of miR-146a-5p (A) and TRAF6 mRNA (B) in the hippocampus of a mouse model of stroke using quantitative reverse transcription-polymerase chain reaction.

Data are expressed as the mean ± SD (n = 6), and were analyzed using nonparametric tests. *P < 0.05, *vs.* sham group; #P < 0.05, *vs.* SE group (Kruskal-Wallis test followed by Mann-Whitney U test). EE group: stroke + enriched environment group; IE group: stroke + isolated environment group; SE group: stroke + standard environment group; TRAF6: tumor necrosis factor receptor-associated factor 6.

Figure 9 | TRAF6 as a target gene of miR-146a-5p according to the database prediction comparison analysis.

There were three potential binding sites of the TRAF6 mRNA 3′ untranslated region to miR-146a-5p according to the principle of base complementary pairing (A=T, C=G). TRAF6: Tumor necrosis factor receptor-associated factor 6.

The EE is an effective rehabilitation therapy. Compared with SEs, EEs provide animals with more space equipped with a variety of toys, and offer more sensations, movement, and social stimulation (Zhang et al., 2021). Social stimulation is recognized as a key factor affecting functional recovery and mortality after stroke (Morris et al., 1990; Hinojosa et al., 2011; Steptoe et al., 2013). Compared with age-matched healthy individuals, stroke survivors experience increased social isolation (Ebrahim et al., 1986). Studies have shown that EE treatment has a neuroprotective effect on animal models of cerebral ischemia (Li et al., 2016) and can improve the learning and memory dysfunction of mice after stroke by promoting plasticity of neuronal circuits (Nithianantharajah and Hannan, 2006) and hippocampal dentate gyrus neurogenesis (Brown et al., 2003). Alternatively, long-term social isolation can increase the risk of vascular and nervous system diseases (Friedler et al., 2015), accelerate the rate of memory decline in older adult people (Bassuk et al., 1999; Ertel et al., 2008), and reduce synaptic plasticity, hippocampal neurogenesis, and spatial cognition (Quan et al., 2010; Kamal et al., 2014; Almeida et al., 2020). In this study, the Morris water maze test was used to detect the effects of different living environments on learning and memory abilities of a mouse model of stroke. We found that in the SE, the post-stroke cognitive function of mice decreased. The EE significantly improved the learning and memory ability of a mouse model of stroke, while the IE aggravates the PSCI of mice.

The hippocampus, located in the temporal lobe of the brain, plays an important role in the formation of normal learning and memory. Previous studies have shown that the hippocampal microstructure of rats will be damaged to varying degrees after stroke (Bettio et al., 2017; Hu et al., 2020). To study the mechanism of the effect of an EE and IE on the behavior of a mouse model of stroke, we first used hematoxylin-eosin and Nissl staining to analyze the pathological morphology of the hippocampal CA1 region of mice in each group, and observed the hippocampal CA1 region with light microscopy. We found that inflammatory damage of neurons appeared in hippocampal CA1 region after stroke in a SE, which led to the decline of learning and memory function. In the EE group, the damaged and inflammatory state of neurons in the hippocampal CA1 region were alleviated, the number of Nissl bodies was restored, and learning and memory ability was improved, which indicates that the EE improves the cognitive function of mice by improving the pathological state of neurons in the hippocampal area. In the IE group, the hippocampal CA1 cells were severely damaged and their structure was unclear; moreover, the number of Nissl bodies was significantly reduced, which indicates that the IE aggravated the pathological damage in the hippocampus of mice after stroke, resulting in more severe cognitive impairment.

Neuroinflammation, especially inflammation in the hippocampus, can lead to cognitive dysfunction (Sun et al., 2017), and is an important pathological mechanism underlying PSCI (Zhang et al., 2021). In recent work, AIM2 inflammasome-mediated inflammation and pyroptosis were found to aggravate PSCI; therefore, it was possible to treat PSCI by targeting and inhibiting inflammation (Kim et al., 2020). The pro-inflammatory cytokines IL-1β, IL-6, and TNF-α are closely associated with learning and memory disorders (Wu et al., 2012), and can lead to cognitive dysfunction by activating different cell signal transduction pathways and interfering with synaptic plasticity and long-term potentiation (Barrientos et al., 2012). TRAF6 is a key binding protein in the inflammatory signaling pathway. Activated by upstream inflammatory stimulation, TRAF6 can interact with IRAK1, promote the nuclear localization and transcriptional activity of NF-κBp65 (Swantek et al., 2000; Flannery and Bowie, 2010; Lee et al., 2016), and further upregulate pro-inflammatory cytokines (such as IL-6 and TNF-α) (Taganov et al., 2006). The present study found that the expression of TRAF6 in the hippocampus of mice in the SE group was upregulated, nuclear NF-κBp65 was increased, the nuclear translocation of NF-κBp65 was significantly increased, and the expression of pro-inflammatory factors (IL-6 and TNF-α) was upregulated, which indicates that the TRAF6/NF-kBp65 signaling pathway is activated and the neuroinflammatory response is enhanced in the hippocampus of mice after stroke. These results are consistent with the above research conclusions.

Studies have shown that EE treatment can reverse hippocampal neuroinflammation (Jurgens and Johnson, 2012) and reduce inflammation after stroke (Gonçalves et al., 2018). In contrast, previous work has reported glial cell activation and increased IL-1β, IL-6, and TNF-α levels in the prefrontal cortex and hippocampus of IE mice (Wang et al., 2018; Alshammari et al., 2020). We found that after EE intervention, the expression of TRAF6 and pro-inflammatory factors (IL-6 and TNF-α) in the hippocampus of a mouse model of stroke was reduced, NF-κBp65 nuclear transport was reduced, and hippocampal neuroinflammation was reversed; however, IE increased the expression of TRAF6/NF-κBp65 signaling pathway proteins in the hippocampus of a mouse model of stroke and aggravated the neuroinflammatory response in the hippocampus. Our results highlight the therapeutic effect of the EE on hippocampal neuroinflammation in a mouse model of stroke, and the IE-induced inflammatory damage to the hippocampus in a mouse model of stroke.

miRNA, a simple type of non-coding single-stranded small RNA, participates in key biological processes, including cell apoptosis, differentiation, proliferation, metastasis, and metabolism (Mens and Ghanbari, 2018; O'Brien et al., 2018). Multiple studies have shown that regulating the expression of miRNA in the brain can improve the functional recovery of mice with ischemic stroke (Geng et al., 2019; Wang et al., 2019). miR-146a is involved in the regulation of neurological diseases and is closely related to neuroinflammation (Fan et al., 2020; Leontariti et al., 2020). In a study of breast cancer cells, Bhaumik et al. (2008) found that inflammatory factors such as TNF-α can trigger the production of miR-146a through NF-κB-dependent pathways. Another study demonstrated that activation of the NF-κBp65 signaling pathway promotes the expression of miR-146a-5p to a certain extent (Lu et al., 2015). Additionally, researchers such as Avenoso et al. (2021) found that during the hyaluronic acid 6-mer-induced inflammatory response, the upregulation of miR146a reduced the inflammatory cascade by regulating the activation of NF-κB. The experimental data revealed that the expression of miR-146a in the hippocampus of the SE group was higher than that in the sham group. We believe that, under normal circumstances, the mouse hippocampal NF-κB signaling pathway and miR-146a are in a relatively stable balance. In the SE group, the increased expression of miR-146a in the hippocampus of mice may be caused by activation of the NF-κB signaling pathway induced by stroke, following which the increase in miR-146a negatively regulates the NF-κB signaling pathway through the targeting effect of TRAF6, which controls neuroinflammation of the hippocampus to a certain extent. Taken together, this process may function as a negative feedback regulation mechanism of the body's anti-inflammatory response. However, the increase in miR-146a caused by stroke is insufficient to prevent the cascade effect of neuroinflammation during stroke. Considering that the role of miRNAs in the regulation of neuroinflammation is complex and dynamic, both pro- and anti-inflammatory miRNAs are often activated in parallel (Gaudet et al., 2018). Therefore, the existence of pro-inflammatory miRNAs that promote neuroinflammation remains a possibility.

Interestingly, studies have found that miRNAs can regulate many aspects of social interaction (Bahi, 2016, 2017; Fregeac et al., 2016). A social environment can also directly affect the expression of miRNAs and, in turn, trigger changes in a number of downstream genes (Ferrante and Conti, 2017; Du et al., 2019). Animal experiments have found that an EE can promote neurogenesis in the dentate gyrus of the hippocampus by regulating the levels of miRNAs in the mouse brain (Brenes et al., 2016). EE can also stimulate endogenous mesenchymal stem cells to secrete exosomes miR-146a, preventing cognitive impairment caused by diabetes (Kubota et al., 2018). Moreover, miR-146a is associated with the neuroinflammatory response (Aronica et al., 2010) and can prevent the decline in cognitive function caused by surgical trauma by inhibiting hippocampal neuroinflammation in a mouse model of postoperative cognitive dysfunction (Chen et al., 2019). TRAF6 is a key signaling molecule in the NF-κB signaling pathway. Through a database comparison and literature analysis (Aronica et al., 2010), we determined that TRAF6 is the target gene of miR-146a-5p. In this study, the level of miR-146a-5p in the hippocampus of the EE group was significantly higher than that of the SE group. Meanwhile, the level of TRAF6 mRNA and protein in the EE group was lower than that of the SE group. These results indicate that the EE intervention-induced increase in miR-146a leads to the degradation of TRAF6 mRNA and inhibits the translation of TRAF6 protein by targeting TRAF6 mRNA. This process may effectively control the activation of the hippocampal NF-κB signaling pathway and the progression of neuroinflammation in a mouse model of stroke, and have a significant protective effect on stroke. Furthermore, studies have also reported that isolated feeding can cause miRNA dysregulation in the brain, as well as decreased hippocampal cell proliferation, leading to poor recovery after stroke (Holmes et al., 2020). In this study, the level of miR-146a in the hippocampus of mice in the IE group was significantly lower than that in the SE group, and the levels of TRAF6 mRNA and protein were significantly higher than those in the SE group. It is possible that the IE reduced the promotion of miR-146a expression caused by activation of NF-κB in the hippocampi of a mouse model of stroke. In

that case, the low level of miR-146a would be unable to inhibit the NF-κB signaling pathway and the cascade amplification effect of inflammation in the hippocampus of mice after stroke by targeting TRAF6, thus aggravating the hippocampal neuroinflammation in mice after stroke.

In summary, EE, a behavioral therapy, has been used in the rehabilitation of various nervous system diseases after years of continuous practice and improvement. In this study, we investigated the effects of an EE and an IE on the cognitive function and hippocampal cell morphology of a mouse model of stroke, and explored the underlying molecular mechanisms of these effects. Our data showed that neuroinflammation occurred in the hippocampus of mice after stroke, the TRAF6/NF-κBp65 signaling pathway was activated, miR-146a-5p expression was up-regulated, and cognitive function was decreased. An IE aggravated hippocampal neuroinflammatory response, nerve damage and cognitive impairment in a mouse model of stroke, which may have been caused by a low level of miR-146a-5p in the hippocampus. However, the EE may increase the expression of miR-146a-5p in the hippocampus of a mouse model of stroke, inhibit TRAF6/NF-κB signaling, reduce the neuroinflammatory response in the hippocampus, alleviate the pathological state of hippocampal damaged nerve cells, and improve cognitive impairment of mice. In conclusion, we found that different living environments can affect hippocampal neuroinflammation and cognitive function in a mouse model of stroke by regulating miR-146a-5p. Thus, miR-146a-5p may represent a potential target for treating PSCI. These findings further explore the mechanism underlying EE-induced improvements in PSCI and could help to develop more effective rehabilitation methods.

In future research, we will extend the intervention cycle of a mouse model of stroke, pay more attention to the effects of the EE at different time points, and study the dynamic changes of various observation indicators. We would also like to explore the relationship between peripheral inflammation and neuroinflammation in a mouse model of stroke; lentiviral miR-146a (agonist/inhibitor) could be injected into the hippocampus of mice to further verify the role of this EE-regulated signaling pathway. In terms of clinical research, we hope to design more complete and enriched rehabilitation programs based on EE elements to better reflect the important role of environmental intervention in clinical practice.

Acknowledgments: *We are grateful for the financial and equipment supports by the Biomedical Research Institute of Northern Jiangsu People's Hospital Affiliated to Yangzhou University, China. We are also grateful for the supports by "Shenzhen Longhua District Rehabilitation Medical Equipment Development and Transformation Joint Key Laboratory" in 2020.*
Author contributions: *Study design: HYZ, XW, ZXM, YPH; literature search: XJ, XJT, JYW, MN; data analysis: PY, NS, and XJT; manuscript writing: HYZ, XW, ZXM, XJ. All authors have approved the final version of the manuscript.*
Conflicts of interest: *The authors declare that there are no conflicts of interest concerning this manuscript.*
Availability of data and materials: *All data generated or analyzed during this study are included in this published article and its supplementary information files.*

Open peer reviewers: *María Esteban, Instituto de Investigacion Biomedica de Salamanca, Spain; Dong Lin, Fujian University of Traditional Chinese Medicine, China.*
Additional file: *Open peer review reports 1 and 2.*

References

Almeida FB, Nin MS, Barros HMT (2020) The role of allopregnanolone in depressive-like behaviors: Focus on neurotrophic proteins. Neurobiol Stress 12:100218.

Alshammari TK, Alghamdi H, Alkhader LF, Alqahtani Q, Alrasheed NM, Yacoub H, Alnaem N, AlNakiyah M, Alshammari MA (2020) Analysis of the molecular and behavioral effects of acute social isolation on rats. Behav Brain Res 377:112191.

Aronica E, Fluiter K, Iyer A, Zurolo E, Vreijling J, van Vliet EA, Baayen JC, Gorter JA (2010) Expression pattern of miR-146a, an inflammation-associated microRNA, in experimental and human temporal lobe epilepsy. Eur J Neurosci 31:1100-1107.

Avenoso A, D'Ascola A, Scuruchi M, Mandraffino G, Campo S, Campo GM (2021) miR146a up-regulation is involved in small HA oligosaccharides-induced pro-inflammatory response in human chondrocytes. Biochim Biophys Acta Gen Subj 1865:129731.

Bahi A (2016) Sustained lentiviral-mediated overexpression of microRNA124a in the dentate gyrus exacerbates anxiety- and autism-like behaviors associated with neonatal isolation in rats. Behav Brain Res 311:298-308.

Bahi A (2017) Hippocampal BDNF overexpression or microR124a silencing reduces anxiety- and autism-like behaviors in rats. Behav Brain Res 326:281-290.

Barrientos RM, Hein AM, Frank MG, Watkins LR, Maier SF (2012) Intracisternal interleukin-1 receptor antagonist prevents postoperative cognitive decline and neuroinflammatory response in aged rats. J Neurosci 32:14641-14648.

Bassuk SS, Glass TA, Berkman LF (1999) Social disengagement and incident cognitive decline in community-dwelling elderly persons. Ann Intern Med 131:165-173.

Bettio LEB, Rajendran L, Gil-Mohapel J (2017) The effects of aging in the hippocampus and cognitive decline. Neurosci Biobehav Rev 79:66-86.

Bezard E, Dovero S, Belin D, Duconger S, Jackson-Lewis V, Przedborski S, Piazza PV, Gross CE, Jaber M (2003) Enriched environment confers resistance to 1-methyl-4-phenyl-1,2,3,6-tetrahydropyridine and cocaine: involvement of dopamine transporter and trophic factors. J Neurosci 23:10999-11007.

Bhaumik D, Scott GK, Schokrpur S, Patil CK, Campisi J, Benz CC (2008) Expression of microRNA-146 suppresses NF-kappaB activity with reduction of metastatic potential in breast cancer cells. Oncogene 27:5643-5647.

Brenes JC, Lackinger M, Höglinger GU, Schratt G, Schwarting RK, Wöhr M (2016) Differential effects of social and physical environmental enrichment on brain plasticity, cognition, and ultrasonic communication in rats. J Comp Neurol 524:1586-1607.

Brown J, Cooper-Kuhn CM, Kempermann G, Van Praag H, Winkler J, Gage FH, Kuhn HG (2003) Enriched environment and physical activity stimulate hippocampal but not olfactory bulb neurogenesis. Eur J Neurosci 17:2042-2046.

Chen L, Dong R, Lu Y, Zhou Y, Li K, Zhang Z, Peng M (2019) MicroRNA-146a protects against cognitive decline induced by surgical trauma by suppressing hippocampal neuroinflammation in mice. Brain Behav Immun 78:188-201.

Du J, Li M, Huang Q, Liu W, Li WQ, Li YJ, Gong ZC (2019) The critical role of microRNAs in stress response: Therapeutic prospect and limitation. Pharmacol Res 142:294-302.

Ebrahim S, Barer D, Nouri F (1986) Use of the Nottingham Health Profile with patients after a stroke. J Epidemiol Community Health 40:166-169.

Ertel KA, Glymour MM, Berkman LF (2008) Effects of social integration on preserving memory function in a nationally representative US elderly population. Am J Public Health 98:1215-1220.

Fan W, Liang C, Ou M, Zou T, Sun F, Zhou H, Cui L (2020) MicroRNA-146a is a wide-reaching neuroinflammatory regulator and potential treatment target in neurological diseases. Front Mol Neurosci 13:90.

Faralli A, Bigoni M, Mauro A, Rossi F, Carulli D (2013) Noninvasive strategies to promote functional recovery after stroke. Neural Plast 2013:854597.

Ferrante M, Conti GO (2017) Environment and neurodegenerative diseases: an update on miRNA role. Microrna 6:157-165.

Flannery S, Bowie AG (2010) The interleukin-1 receptor-associated kinases: critical regulators of innate immune signalling. Biochem Pharmacol 80:1981-1991.

Fregeac J, Colleaux L, Nguyen LS (2016) The emerging roles of microRNAs in autism spectrum disorders. Neurosci Biobehav Rev 71:729-738.

Friedler B, Crapser J, McCullough L (2015) One is the deadliest number: the detrimental effects of social isolation on cerebrovascular diseases and cognition. Acta Neuropathol 129:493-509.

Gaudet AD, Fonken LK, Watkins LR, Nelson RJ, Popovich PG (2018) MicroRNAs: roles in regulating neuroinflammation. Neuroscientist 24:221-245.

Geng W, Tang H, Luo S, Lv Y, Liang D, Kang X, Hong W (2019) Exosomes from miRNA-126-modified ADSCs promotes functional recovery after stroke in rats by improving neurogenesis and suppressing microglia activation. Am J Transl Res 11:780-792.

Gonçalves LV, Herlinger AL, Ferreira TAA, Coitinho JB, Pires RGW, Martins-Silva C (2018) Environmental enrichment cognitive neuroprotection in an experimental model of cerebral ischemia: biochemical and molecular aspects. Behav Brain Res 348:171-183.

Hinojosa R, Haun J, Hinojosa MS, Rittman M (2011) Social isolation poststroke: relationship between race/ethnicity, depression, and functional independence. Top Stroke Rehabil 18:79-86.

Hockly E, Cordery PM, Woodman B, Mahal A, van Dellen A, Blakemore C, Lewis CM, Hannan AJ, Bates GP (2002) Environmental enrichment slows disease progression in R6/2 Huntington's disease mice. Ann Neurol 51:235-242.

Holmes A, Xu Y, Lee J, Maniskas ME, Zhu L, McCullough LD, Venna VR (2020) Post-stroke social isolation reduces cell proliferation in the dentate gyrus and alters miRNA profiles in the aged female mice brain. Int J Mol Sci 22:99.

Hu J, Li C, Hua Y, Liu P, Gao B, Wang Y, Bai Y (2020) Constraint-induced movement therapy improves functional recovery after ischemic stroke and its impacts on synaptic plasticity in sensorimotor cortex and hippocampus. Brain Res Bull 160:8-23.

Jurgens HA, Johnson RW (2012) Environmental enrichment attenuates hippocampal neuroinflammation and improves cognitive function during influenza infection. Brain Behav Immun 26:1006-1016.

Kamal A, Ramakers GM, Altinbilek B, Kas MJ (2014) Social isolation stress reduces hippocampal long-term potentiation: effect of animal strain and involvement of glucocorticoid receptors. Neuroscience 256:262-270.

Kim H, Seo JS, Lee SY, Ha KT, Choi BT, Shin YI, Ju Yun Y, Shin HK (2020) AIM2 inflammasome contributes to brain injury and chronic post-stroke cognitive impairment in mice. Brain Behav Immun 87:765-776.

Kovesdi E, Gyorgy AB, Kwon SK, Wingo DL, Kamnaksh A, Long JB, Kasper CE, Agoston DV (2011) The effect of enriched environment on the outcome of traumatic brain injury; a behavioral, proteomics, and histological study. Front Neurosci 5:42.

Kubota K, Nakano M, Kobayashi E, Mizue Y, Chikenji T, Otani M, Nagaishi K, Fujimiya M (2018) An enriched environment prevents diabetes-induced cognitive impairment in rats by enhancing exosomal miR-146a secretion from endogenous bone marrow-derived mesenchymal stem cells. PLoS One 13:e0204252.

Labat-gest V, Tomasi S (2013) Photothrombotic ischemia: a minimally invasive and reproducible photochemical cortical lesion model for mouse stroke studies. J Vis Exp:50370.

Lee HM, Kim TS, Jo EK (2016) MiR-146 and miR-125 in the regulation of innate immunity and inflammation. BMB Rep 49:311-318.

Leontariti M, Avgeris M, Katsarou MS, Drakoulis N, Siatouni A, Verentzioti A, Alexoudi A, Fytraki A, Patrikelis P, Vassilacopoulou D, Gatzonis S, Sideris DC (2020) Circulating miR-146a and miR-134 in predicting drug-resistant epilepsy in patients with focal impaired awareness seizures. Epilepsia 61:959-970.

Li YW, Li QY, Wang JH, Xu XL (2016) Contribution of p38 MAPK to the ameliorating effect of enriched environment on the cognitive deficits induced by chronic cerebral hypoperfusion. Cell Physiol Biochem 40:549-557.

Lu Y, Cao DL, Jiang BC, Yang T, Gao YJ (2015) MicroRNA-146a-5p attenuates neuropathic pain via suppressing TRAF6 signaling in the spinal cord. Brain Behav Immun 49:119-129.

Lukiw WJ, Zhao Y, Cui JG (2008) An NF-kappaB-sensitive micro RNA-146a-mediated inflammatory circuit in Alzheimer disease and in stressed human brain cells. J Biol Chem 283:31315-31322.

Maresova P, Tomsone S, Lameski P, Madureira J, Mendes A, Zdravevski E, Chorbev I, Trajkovik V, Ellen M, Rodile K (2018) Technological solutions for older people with Alzheimer's disease: review. Curr Alzheimer Res 15:975-983.

Mens MMJ, Ghanbari M (2018) Cell cycle regulation of stem cells by microRNAs. Stem Cell Rev Rep 14:309-322.

Mijajlović MD, Pavlović A, Brainin M, Heiss WD, Quinn TJ, Ihle-Hansen HB, Hermann DM, Assayag EB, Richard E, Thiel A, Kliper E, Shin YI, Kim YH, Choi S, Jung S, Lee YB, Sinanović O, Levine DA, Schlesinger I, Mead G, et al. (2017) Post-stroke dementia- a comprehensive review. BMC Med 15:11.

Morris PL, Robinson RG, Raphael B (1990) Prevalence and course of depressive disorders in hospitalized stroke patients. Int J Psychiatry Med 20:349-364.

Narasimhalu K, Lee J, Leong YL, Ma L, De Silva DA, Wong MC, Chang HM, Chen C (2015) Inflammatory markers and their association with post stroke cognitive decline. Int J Stroke 10:513-518.

Ngandu T, Lehtisalo J, Solomon A, Levälahti E, Ahtiluoto S, Antikainen R, Bäckman L, Hänninen T, Jula A, Laatikainen T, Lindström J, Mangialasche F, Paajanen T, Pajala S, Peltonen M, Rauramaa R, Stigsdotter-Neely A, Strandberg T, Tuomilehto J, Soininen H, et al. (2015) A 2 year multidomain intervention of diet, exercise, cognitive training, and vascular risk monitoring versus control to prevent cognitive decline in at-risk elderly people (FINGER): a randomised controlled trial. Lancet 385:2255-2263.

Nithianantharajah J, Hannan AJ (2006) Enriched environments, experience-dependent plasticity and disorders of the nervous system. Nat Rev Neurosci 7:697-709.

O'Brien J, Hayder H, Zayed Y, Peng C (2018) Overview of microRNA biogenesis, mechanisms of actions, and circulation. Front Endocrinol (Lausanne) 9:402.

Oeckinghaus A, Ghosh S (2009) The NF-kappaB family of transcription factors and its regulation. Cold Spring Harb Perspect Biol 1:a000034.

Park SH, Seo JH, Kim YH, Ko MH (2014) Long-term effects of transcranial direct current stimulation combined with computer-assisted cognitive training in healthy older adults. Neuroreport 25:122-126.

Quan MN, Tian YT, Xu KH, Zhang T, Yang Z (2010) Post weaning social isolation influences spatial cognition, prefrontal cortical synaptic plasticity and hippocampal potassium ion channels in Wistar rats. Neuroscience 169:214-222.

Restivo L, Ferrari F, Passino E, Sgobio C, Bock J, Oostra BA, Bagni C, Ammassari-Teule M (2005) Enriched environment promotes behavioral and morphological recovery in a mouse model for the fragile X syndrome. Proc Natl Acad Sci U S A 102:11557-11562.

Sachdev PS, Brodaty H, Valenzuela MJ, Lorentz L, Looi JC, Berman K, Ross A, Wen W, Zagami AS (2006) Clinical determinants of dementia and mild cognitive impairment following ischaemic stroke: the Sydney Stroke Study. Dement Geriatr Cogn Disord 21:275-283.

Schmittgen TD, Livak KJ (2008) Analyzing real-time PCR data by the comparative C(T) method. Nat Protoc 3:1101-1108.

Schneider CA, Rasband WS, Eliceiri KW (2012) NIH Image to ImageJ: 25 years of image analysis. Nat Methods 9:671-675.

Steptoe A, Shankar A, Demakakos P, Wardle J (2013) Social isolation, loneliness, and all-cause mortality in older men and women. Proc Natl Acad Sci U S A 110:5797-5801.

Sun JH, Tan L, Yu JT (2014) Post-stroke cognitive impairment: epidemiology, mechanisms and management. Ann Transl Med 2:80.

Sun L, Dong R, Xu X, Yang X, Peng M (2017) Activation of cannabinoid receptor type 2 attenuates surgery-induced cognitive impairment in mice through anti-inflammatory activity. J Neuroinflammation 14:138.

Swantek JL, Tsen MF, Cobb MH, Thomas JA (2000) IL-1 receptor-associated kinase modulates host responsiveness to endotoxin. J Immunol 164:4301-4306.

Taganov KD, Boldin MP, Chang KJ, Baltimore D (2006) NF-kappaB-dependent induction of microRNA miR-146, an inhibitor targeted to signaling proteins of innate immune responses. Proc Natl Acad Sci U S A 103:12481-12486.

Teo WP, Muthalib M, Yamin S, Hendy AM, Bramstedt K, Kotsopoulos E, Perrey S, Ayaz H (2016) Does a combination of virtual reality, neuromodulation and neuroimaging provide a comprehensive platform for neurorehabilitation?- A narrative review of the literature. Front Hum Neurosci 10:284.

Uzdensky AB (2018) Photothrombotic stroke as a model of ischemic stroke. Transl Stroke Res 9:437-451.

Wang L, Cao M, Pu T, Huang H, Marshall C, Xiao M (2018) Enriched physical environment attenuates spatial and social memory impairments of aged socially isolated mice. Int J Neuropsychopharmacol 21:1114-1127.

Wang X, Chen A, Wu H, Ye M, Cheng H, Jiang X, Wang X, Zhang X, Wu D, Gu X, Shen F, Shan C, Yu D (2016) Enriched environment improves post-stroke cognitive impairment in mice by potential regulation of acetylation homeostasis in cholinergic circuits. Brain Res 1650:232-242.

Wang Z, Yuan Y, Zhang Z, Ding K (2019) Inhibition of miRNA-27b enhances neurogenesis via AMPK activation in a mouse ischemic stroke model. FEBS Open Bio 9:859-869.

Watson BD, Dietrich WD, Busto R, Wachtel MS, Ginsberg MD (1985) Induction of reproducible brain infarction by photochemically initiated thrombosis. Ann Neurol 17:497-504.

White JH, Bartley E, Janssen H, Jordan LA, Spratt N (2015) Exploring stroke survivor experience of participation in an enriched environment: a qualitative study. Disabil Rehabil 37:593-600.

Will B, Galani R, Kelche C, Rosenzweig MR (2004) Recovery from brain injury in animals: relative efficacy of environmental enrichment, physical exercise or formal training (1990-2002). Prog Neurobiol 72:167-182.

Wu X, Lu Y, Dong Y, Zhang G, Zhang Y, Xu Z, Culley DJ, Crosby G, Marcantonio ER, Tanzi RE, Xie Z (2012) The inhalation anesthetic isoflurane increases levels of proinflammatory TNF-α, IL-6, and IL-1β. Neurobiol Aging 33:1364-1378.

Xie H, Yu K, Zhou N, Shen X, Tian S, Zhang B, Wang Y, Wu J, Liu G, Jiang C, Hu R, Ayata C, Wu Y (2019) Enriched environment elicits proangiogenic mechanisms after focal cerebral ischemia. Transl Stroke Res 10:150-159.

Zhang X, Bi X (2020) Post-stroke cognitive impairment: a review focusing on molecular biomarkers. J Mol Neurosci 70:1244-1254.

Zhang X, Yuan M, Yang S, Chen X, Wu J, Wen M, Yan K, Bi X (2021) Enriched environment improves post-stroke cognitive impairment and inhibits neuroinflammation and oxidative stress by activating Nrf2-ARE pathway. Int J Neurosci 131:641-649.

P-Reviewers: Esteban M, Lin D; C-Editor: Zhao M; S-Editors: Yu J, Li CH; L-Editors: Cason N, Yu J, Song LP; T-Editor: Jia Y